MODELLING THE POSTBUCKLING BEHAVIOUR OF IMPACTED COMPOSITE AEROSTRUCTURES

Paola Apruzzese†, Brian G. Falzon‡*, Robin Olsson↑
†Department of Aeronautics, Imperial College London, London, UK; ‡Department of
Mechanical and Aerospace Engineering, Monash University, Clayton, Australia;
↑Swerea SICOMP AB, Sweden
* brian.falzon@eng.monash.edu.au

SUMMARY

Two approaches to modelling the effects of embedded defects and impact damage in composite aerostructures are presented. These differ in the manner in which the damage is represented; one as an equivalent delamination and the other as a soft inclusion with non-linear homogenized material properties. These techniques are applied to study the effects of defects and impact damage on the performance of composite panels.

Keywords: impact damage, postbuckling, stiffened panel, delamination, soft inclusion.

INTRODUCTION

A major challenge in developing a reliable virtual testing capability for composite structures is predicting damage growth and its effect on structural performance. This work aims at developing such a capability which will allow the design of advanced composite aerostructures where damage growth is arrested prior to significant structural degradation.

In this paper, two different approaches to model the effects of defects and impact damage are discussed. These are modelled as equivalent delaminations or as soft inclusions. The aim is not to accurately simulate all the events leading to catastrophic failure but rather to provide an estimate of the progressive stiffness reduction of the structure caused by defects and impact damage and subsequently determine the maximum applied strain that a structure can carry prior to significant damage propagation leading to final failure.

IMPACT DAMAGE MODELLED AS AN EQUIVALENT DELAMINATION

Among several forms of damage, induced by low-velocity impact, delamination is undoubtedly one of the most critical. Impact damage is usually characterized by multiple delaminations through the thickness. Delaminations location and dimensions depend mainly on the span-to-thickness ratio of the impacted plate and on the impact energy. The mechanical performance of composite materials can be drastically reduced in the presence of a delamination, in particular, the compressive strength may be reduced by up to 60%.

An accurate study of the effects of impact damage, or even just of an embedded delamination, often necessitates a full 3D analysis. However, such an analysis requires substantial computational resources and entails considerable modelling complexity, making it inappropriate for use early in the design cycle. In order to reduce computational costs, the shell-to-solid coupling technique was used to model the effects of an embedded delamination.

I-stringer composite panel containing bay impact damage modelled as equivalent delamination

This section presents the numerical predictions for two I-stiffened panels with a circular delamination, representing impact damage and an embedded defect, respectively. The panels considered were tested as part of the EDAVCOS program (Efficient Design and Verification of Composite Structures) [1, 2] and contained detailed fractographic analysis of the effects of impact damage and embedded defects in CFRP skin/stringer panels under monotonic compressive loading. The panels were fabricated from Fibredux HTA/6376C CFRP prepreg. The material properties are reported in Table 1 while the panel geometry and stacking sequence are depicted in Figure 1. One of the panels, referred to as SFN1, contained a 15J impact in the bay causing a projected damage area of 381 mm^2 ($\approx$22 mm diameter). A second panel, SFN3, contained a 40 mm diameter ($\approx$1199 mm^2 area) embedded defect (PTFE 10 µm film) located between plies 4 and 5 (90º/+45º) closest to the stiffener foot.
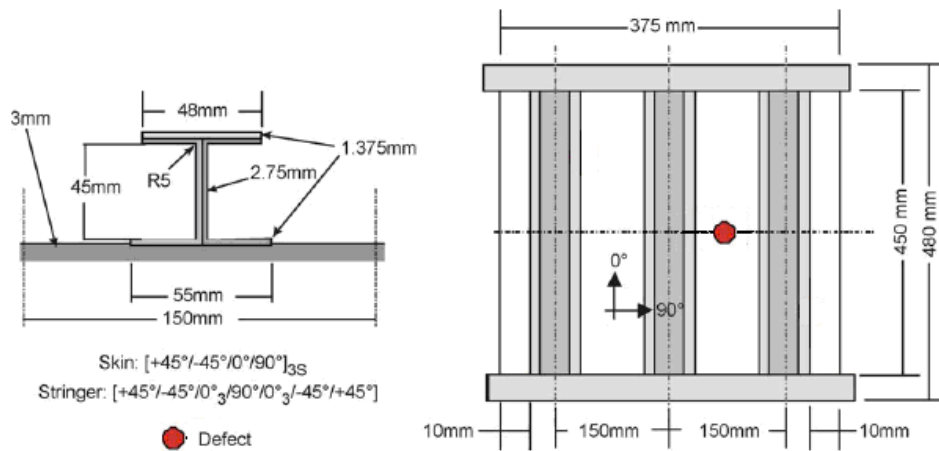

Figure 1 Panel configuration and dimensions

The panels were modelled using the commercial finite element code ABAQUS\Standard. Eight-node continuum shell elements were used to discretize the solid region whilst four-node shell elements were used to model the rest of the panel. The solid region had dimensions L x W x t = 80 mm x 80 mm x 3.3 mm for the SFN3 panel and L x W x t = 44 mm x 44 mm x 3.3 mm for the SFN1 panel.

Impact damage tolerance in laminated structures is often governed by delamination growth. To efficiently assess the damage tolerance of panel SFN1, the critical delamination was identified at the fourth ply interface (closest to the stiffeners) [3]. The

impact damage in panel SFN1 was subsequently modelled as a 22 mm diameter delamination located at the fourth ply interface.

Table 1: Material properties HTA/6376C

Material properties	Value
Longitudinal Young's modulus, E_1	146 GPa
Transverse Young's modulus, E_2	10.5 GPa
Out-of-plane Young's modulus, E_3	10.5 GPa
Out-of-plane shear modulus, G_{13}	5.25 GPa
Out-of-plane shear modulus, G_{23}	3.48 GPa
Poisson's ratio, $\nu_{12} = \nu_{13}$	0.3
Poisson's ratio, ν_{23}	0.51
Ply thickness, t	0.125 mm

The final failure for both panels was overall global skin buckling due to skin/stiffener separation. The final failure load was not predicted by the models since it did not include interface elements at the skin/stiffener interfaces.

For both panels, a layer of cohesive elements was inserted between the 4th and 5th ply closest to the stiffener face and used to simulate the delamination growth. An initial imperfection based on a linear combination of the first two eigenvectors with maximum amplitude of 1% of the skin thickness was added to the perfect geometry of the panel. The non-linear analysis was performed using the Newton-Raphson method.

Figure 2 reports the reaction force versus applied end-displacement for panel SFN3. Excellent agreement was found in the slope of the equilibrium curve and in the initial buckling load.
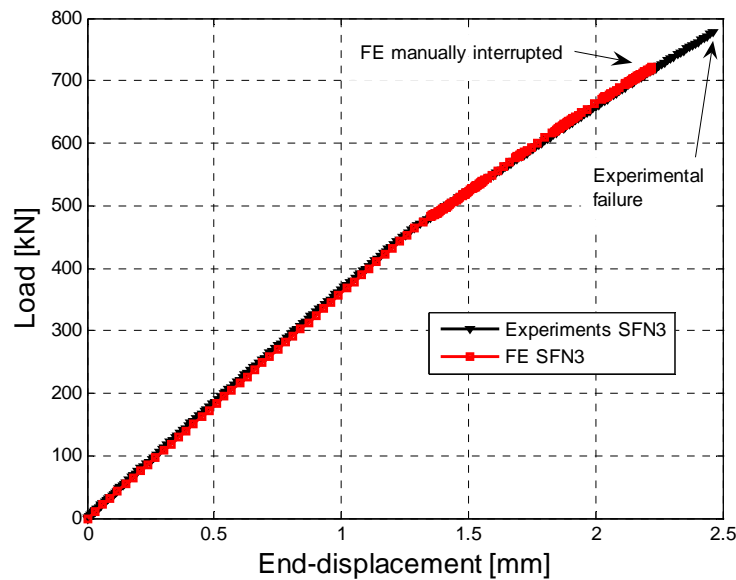

Figure 2 Load versus end-displacement comparison for the SFN3 panel.

Figure 3 shows a comparison between computed and experimentally observed deflections at the centre of the delaminated region as a function of the reaction forces

for the SFN3 panel. No experimental data was available for the lower sublaminate out-of-plane defection. The experimental results show some initial out-of-plane deflection in the skin. This was attributed to the presence of the insert where previous experimental studies have shown the sublaminate, above this insert, behaving like an arch where the insert is wedged in at the boundary. This initial deflection was not taken into account in the numerical model. As shown in Figure 3, a fairly good agreement with the experimental results is found in both the initial buckling of the upper sub-laminate (point A) and the initial buckling of the skin (point B).
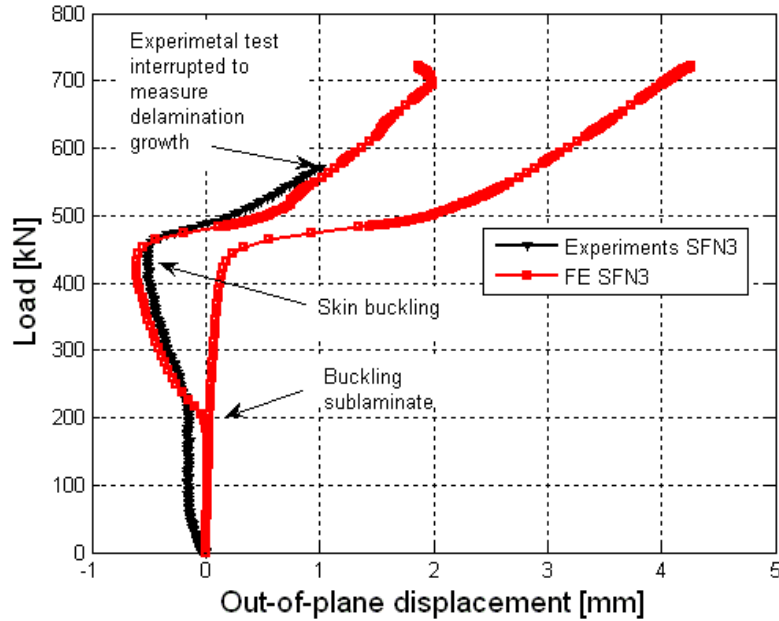

Figure 3 Load versus out-of-plane displacement comparison for the SFN3 panel.

Figure 4 shows the damage growth in the cohesive element layer at an applied strain of 4750 $\mu\varepsilon$. Note that the direction of propagation is not symmetric and is inclined with respect to the loading condition. This is consistent with the experimental findings where the delamination growth consisted of unsymmetrical lobes growing at approximately 75° transverse to the applied load [2].

In the case for the SFN1 panel, no upper sublaminate buckling occurred and damage growth was relatively limited prior to failure, although there was some evidence of a slight increase in the damage width as the applied strain increased. The rate of damage growth increased with applied strain, reaching an increase in area of 22% at the final measurement, about -300 $\mu\varepsilon$ prior to failure. In the SFN1 test the buckle mode changed from three to four half waves in each bay. Since none of the other panels of the EDAVCOS series exhibited such behaviour, the mode switch was attributed to the presence of the impact damage.

Figure 5 shows a comparison between the experimental and numerically predicted reaction force versus applied end-displacement, while Figure 6 shows the reaction force versus out-of-plane displacements. For the SFN1 panel the initial buckling load of the skin was slightly overestimated and the mode switch was not predicted by the model.

This might be due to the simplifications introduced into the model to model impact damage as only one delamination at the fourth ply interface was modelled. In fact, a further delamination at the 0°//90° interface closest to the middle of the laminate thickness was found to have also grown. Interaction with other forms of damage, e.g. other delaminations, matrix cracking or fibre failure, may influence the response. Finally, low velocity impacts usually cause a permanent deflection (indentation) in the laminate. The indentation by itself introduces an initial imperfection which might have triggered the mode switch. Consistent with experimental observations, delamination growth in the model was very limited up to an applied strain of 4800 µε) .
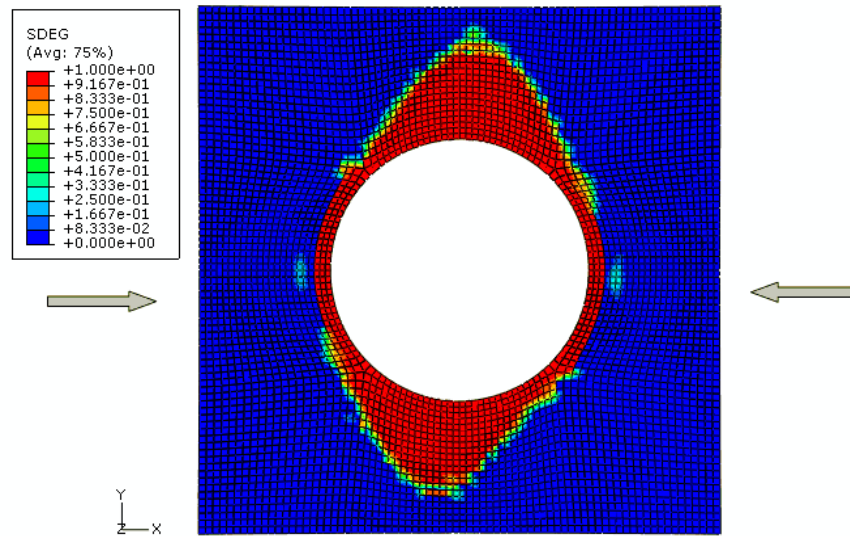

Figure 4 Delamination growth SFN3 panel.

The examples above demonstrate that modelling embedded delaminations is reliable in predicting the effects of such defects on the performance of stiffened structures. However for the case of impact damage the predicted response was less reliable, for example, no mode switch was predicted although the overall response of failure by the sudden onset of damage propagation was captured. A better prediction of the effects of impact damage, on the performance of a composite structure, requires methods that also consider the influence of stiffness reduction in the damaged zone. A method of representing this stiffness reduction is illustrated in the following section.

IMPACT DAMAGE MODELLED AS A SOFT INCLUSION

The knowledge of the constitutive properties in the damage zone is crucial for a reliable failure prediction. Attempts to predict the strength after impact have been based on the concept of an equivalent hole [4] or soft inclusions approach [5-7], as well as more complex models involving single [8] and multiple delaminations [9]. The soft inclusion method represents impact damage by replacing a section of the composite laminate with an inclusion (normally circular or elliptical in shape) having reduced material properties to match those of an impact damage region. The major deficiency of soft inclusion models is the lack of knowledge of the actual stiffness of impact damage zones. Stiffness reductions are primarily connected to fibre fracture, which is concentrated in

the centre of the damage zone. Thus, the constitutive behaviour within the damage zone may not only be non-linear but also non-uniform.

Recently a new technique to predict the stiffness reduction of the impacted area has been developed in the Department of Aeronautics at Imperial College London [10, 11]. This technique, in the following referred as the *inverse method*, is based on iteratively updating the material properties in an FE model to match the displacements in the model to optically measured displacement fields in a damaged specimen under load [10,11]. In tension the reduction in the elastic modulus is shown to be confined to small regions with fibre damage in the center of the damage zone and the modulus usually decreases towards the center of the damage zone [10]. In compression, the behaviour of the damage region is influenced by both material damage and local delamination buckling. Thus, the variations in the elastic modulus in the damage region computed by the *inverse method* no longer correspond to true variations in material stiffness only but to the combined effect of damage and local buckling. Consequently, the soft inclusion with non-linear material properties evaluated with the *inverse method* has to be regarded as an inclusion which takes into account both damage evolution and local buckling [11].
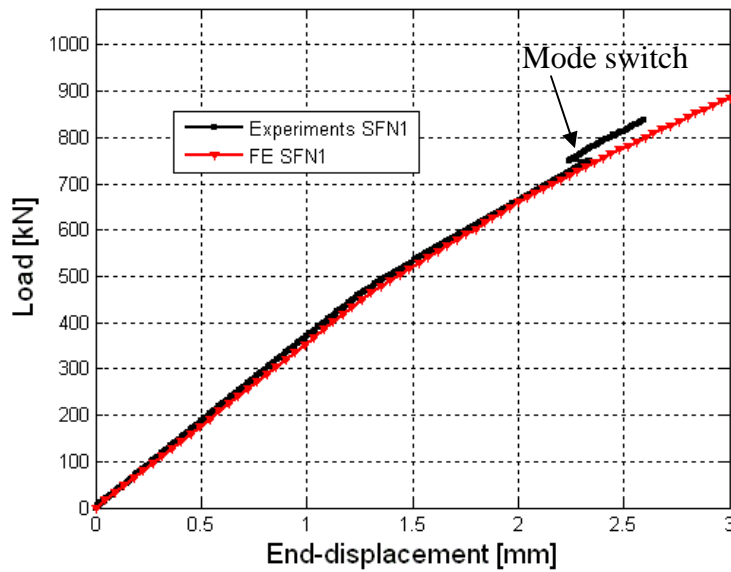

Figure 5 Load versus end-displacement comparison for the SFN1 panel.

In this paper a numerical model to represent impact damage as a soft inclusion with nonlinear material properties, as provided by the *inverse method,* is presented. The goal of this approach is to provide an estimate of the maximum applied strain that a structure can carry prior to significant damage propagation leading to final failure.

Numerical model of the soft inclusion

The impact damage region is modelled as a series of concentric elliptical/circular sub-regions with independent non-linear elastic homogenized material properties which deteriorate with applied strain, as provided by the *inverse method.*

Each in-plane elastic coefficient (E_x, E_y, G_{xy}, ν_{xy}) is defined by a non-linear elastic law as a function of the local strains (different laws in tension ($\varepsilon_x > 0$) and compression ($\varepsilon_x <$

0) can be defined). In particular, each material property is defined as a polynomial function, $f_{T,C}^n$, of an appropriate local strain, that is, $E_x = f_{T,C}^n(\varepsilon_x)$, $E_y = f_{T,C}^n(\varepsilon_y)$, $G_{xy} = f_{T,C}^n(\gamma_{xy})$, and the Poisson's ratio, $v_{xy} = f_{T,C}^n(\varepsilon_x)$, where the superscript n is the order of the polynomial used to interpolate the experimental data and the subscript T and C refer to tensile and compressive longitudinal strain, respectively. v_{yx} follows by applying the (elastic) convention: $E_x/v_{xy} = E_y/v_{yx}$.
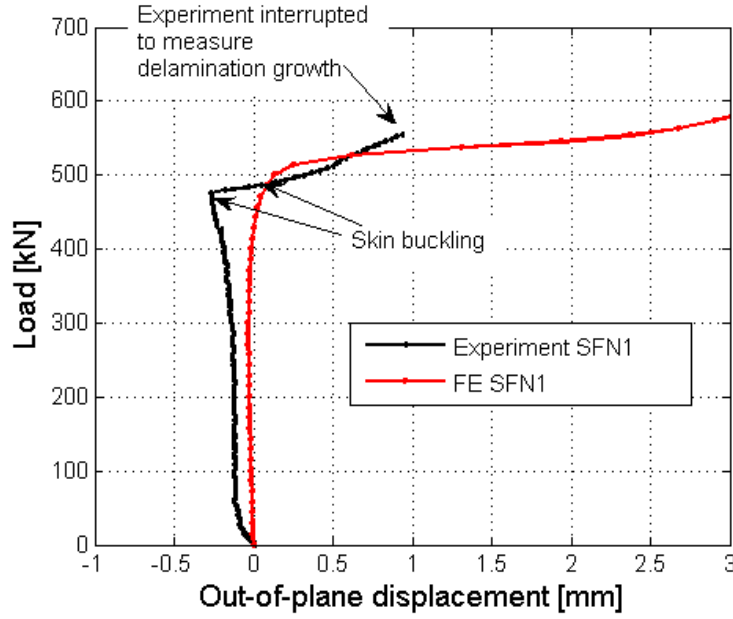

Figure 6 Reaction force versus out-of-plane displacement SFN1.

Figure 7 shows the degradation of the Young's modulus, E_x, with the applied strain as obtained by the *inverse method*. Once the maximum strain (local failure strain) is exceeded, the correspondent material properties are reduced to zero. The material properties provided by the *inverse method* are homogenized throughout the thickness (i.e. damage averaged over the thickness). However, impacted regions are rarely homogeneous through the thickness and this variation has been shown to influence the response of the structure [12] In order to take into account the variation through the thickness, the damage may be sectioned through the thickness. The material property functions in each section are then scaled with respect to the severity of the damage. Both the thickness and the severity of the damage of each section are user defined. The material properties are scaled at each local strain using a bilinear/linear interpolation of the data provided by the inverse method, see Appendix A.

The non-linear material model was implemented in ABAQUS/Standard through the user material subroutine (UMAT). The subroutine is called at all integration points within the elements for which the material definition includes the user-defined material behaviour. The user material subroutine takes as input the material constants defined in an ASCII file. The model was implemented in an implicit incremental iterative scheme. The material properties evolution is a function of the applied strains. As a result, at each strain increment, $\Delta\varepsilon$, the new material properties, E_x, E_y, G_{xy} and v_{xy}, are computed and

the stiffness tensor, C, is updated. The new stress state vector, σ^{n+1}, is then computed using the updated stiffness tensor, C^{n+1}.
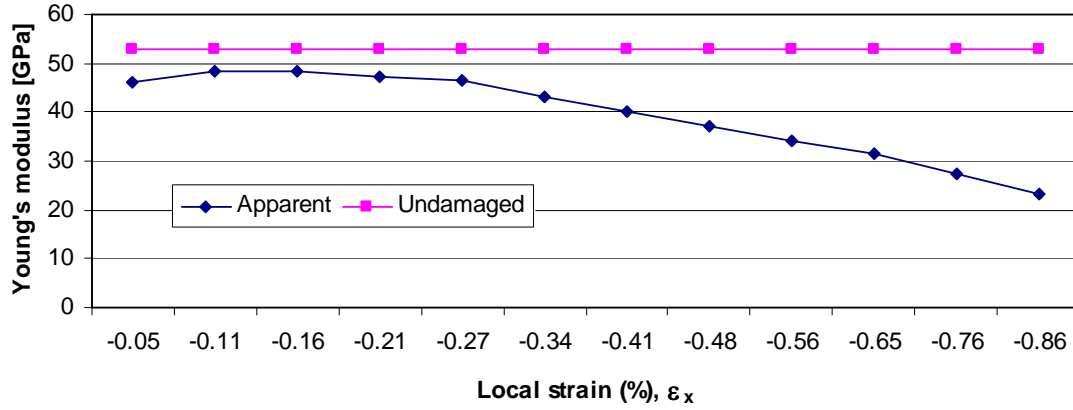

Figure 7 Degradation Young's modulus with the applied strain.

The following example illustrates the capability of the model to capture the response of a damaged composite stiffened panel. However, no experimental data was available to validate the model implemented. Therefore, the following serves to demonstrate the implementation of the model and to show how the impact damage may be represented in the FE model.

I-stiffened panel containing bay impact damage modelled as soft inclusion

The soft inclusion material model was applied to simulate the effects of mid-bay impact damage on the postbuckling behaviour of a stiffened composite panel. Full field displacement measurements necessary for application of the inverse method were not available for the EDAVCOS SFN1 stiffened panels. For this reason the approach to combine a stiffened panel with a soft inclusion was explored in an FE model of a modified SFN1 panel where the skin of the panel was replaced with a quasi-isotropic laminate that had been experimentally impacted at 14J, loaded in compression and analyzed using the inverse approach in [10, 11]. This particular laminate had a thickness of 4.28 mm and was manufactured from Hexcel AS4/8552 carbon/epoxy prepreg with the lay-up $[(0°/±45°/90°)_s/(90°/±45°/0°)_s]_2$. The homogenized undamaged laminate properties were $E_x = E_y = 53.0$GPa, $G_{xy} = 18.4$GPa, and $\nu_{xy} = \nu_{yx} = 0.313$. The C-scan revealed that the impact damage was fairly circular with a diameter of 32mm [11]. The compression test was performed in a modified Boeing anti-buckling rig (100x150 mm specimens with 94 mm free buckling width).

Due to the lack of a fully comparable experiment the main goals of the simulation were to explore the soft inclusion modelling approach in a stiffened panel and to qualitatively assess the failure phenomena in the damage zone.

The FE model of the I-stringers panel was composed of 5747 four-node shell elements with reduced integration and a large-strain formulation. The mesh size in the impact damage region was 1mm, while the global mesh size was 5mm. Based on the

experimental observations, the impact damage was modeled as a circular region with a diameter of 32mm located in the middle of the bay. The elastic material properties and the coefficients of the 3rd order polynomials describing the non-linear variation of the material properties in the impacted region, were introduced by 47 user defined material constants, while the constitutive law was defined through the user material subroutine UMAT. A full non-linear analysis was carried out using the modified Newton-Raphson method. The first element to exceed the maximum local longitudinal strain was located in the middle of the bay (in the longitudinal direction) closest to the central stiffener. Further increases in the applied strain induced a rapid diffusion of the damage (i.e. exceeded maximum strain) in the entire soft inclusion region. At that point the simulation was interrupted. Figure 8 shows the extension of the failure zone a few increments before the simulation was interrupted. SDV1 is a flag that assumes value 0 for $\varepsilon_x < \varepsilon_{xmax}$, where ε_{xmax} is the local failure strain, and 1 when $\varepsilon_x > \varepsilon_{xmax}$. While model verification was established, validation of the model against experimental results was not possible due to the lack of experimental data.
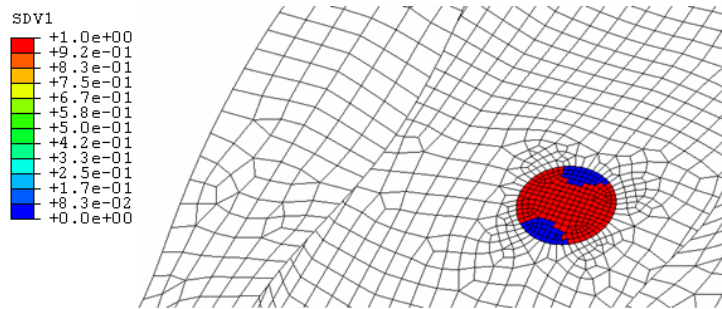

Figure 8 Failure extensions in the soft inclusion region.

CONCLUSIONS

This paper presented two approaches to model the effects of impact damage in composite structures. The first method proved to be accurate in predicting the behaviour of a panel with embedded delamination (i.e. due to fabrication defects) in terms of both initial local buckling of the delaminated area and initial buckling of the skin; the results in the case for the impact damaged panel were not reliable as no mode switch was predicted. However, the model predicted delamination growth just before failure of the panel which is in agreement with the experimental observations. The two examples demonstated that a representative critical delamination may be sufficient when the delamination growth is governed by local buckling of the sublaminates and the damage has small influence on the global buckling. The approach with a single critical delamination is clearly insufficient when the impact damage and its local buckling affects the global skin buckling. The second method (impact damage as soft inclusion) was explored through an FE model of a stiffened panel. No comparison with experimental results was possible due to the lack of experimental data. For a validation of this methodology additional experimental tests on composite stiffened panels are necessary. Future models should also include flatness imperfections after impact, which are know to be important.

ACKNOWLEDGEMENTS

References

1. E. Greenhalgh, C. Meeks, A. Clarke, and J Thatcher. The effect of defects on the performance of post-buckled CFRP stringer-stiffened panels. Composites: Part A, 34:623-633, 2003.

2. C. Meeks, E. Greenhalgh, and B.G. Falzon. Stiffener debonding mechanisms in postbuckled CFRP aerospace panels. Composites Part A: Applied Science and Manufacturing, 36:934-946, 2005.

3. L. Asp. Analysis/test correlation for the FFA DEBUGS prediction and SAAB/FFA/NLR panel tests. FFAP H-1437. The Aeron. Res. Inst. of Sweden. Bromma, 2000.

4. VJ. Hawyes, PT. Curtis, and C. Soutis. Effect of impact damage on the compressive response of composites laminates. Composites: Part A: Applied Science and Manufacturing, 32(9):1263-1270, 2001.

5. T. Nyman, A. Bredberg, and J. Schön. Equivalent damage and residual strength for impact damaged composite structures. Journal of Reinforced Plastics and Composites, 19(6):428-448, 2000.

6. Y. Xiong, C. Poon, Straznicky PV, and Vietinghoff H. A prediction method for the compressive strength of impact damaged composite laminates. Composite & Structures, 30(4):357-367, 1995.

7. L. Zeng and R. Olsson. Buckling induced delamination analysis of composite laminates with soft inclusion. Technical report, FOI-R-0412-SE, FOI - Swedish Defence Research Agency, Stockholm, 2002.

8. K-F. Nilsson, LE. Asp, and A. Sjögren. On transition of delamination growth behaviour for compression loaded composite panels. Int. J Solids Structures, 38(46-47):8407-8440, 2001.

9. H. Suemasu, T. Kumagai, and K. Gozu. Compressive behaviour of multiply delaminated composite laminates, parts 1-2. AIAA J, 36(7):1279-90, 1998.

10. P. Sztefek and R. Olsson. Tensile stiffness distribution in impacted composite laminates determined by an inverse method. Composites Part A: Applied Science and Manufacturing, 39(8):1282-1293, 2008.

11. P. Sztefek and R. Olsson R. Nonlinear compressive stiffness in impacted composite laminates determined by an inverse method. Composites Part A, 40(3):260-272, 2009.

12. R. Olsson, L.E. Asp, S. Nilsson, A. Sjögren. A review of some key developments in the analysis of the effects of impact upon composite structures.

Composite Structures: Theory and Practice. ASTM STP 1383. Grant P, Rousseau C, Eds. West Conshohocken: ASTM: 12-28, 2000.

APPENDIX A

Example scaling material properties through the thickness

Let E_{x0}=53800 MPa be the longitudinal elastic modulus of the undamaged homogenized material (damage d_0=0) and E_{xf} =0 MPa the elastic modulus of a material fully damaged (d_f=1); given the value of the longitudinal elastic modulus in the outer ellipse at a given local strain $\bar{\varepsilon}_x$, $\bar{E}_x(\bar{\varepsilon}_x)$, the average damage in this section in longitudinal direction is

$$d_{xavg}(\bar{\varepsilon}_x) = \frac{\bar{E}_x(\bar{\varepsilon}_x)}{E_x^0} \tag{A1}$$

Let's here assume d_{xavg}=0.45. We want to evaluate the longitudinal elastic modulus, E_x, of the outer ellipse in the three sections through the thickness, section O1, O2, O3 in Figure A1, having d_{x1}=0.7, d_{x2}=0.5 and d_{x3}=0.15, respectively (note: the average damage through the thickness is still d_{xavg}).
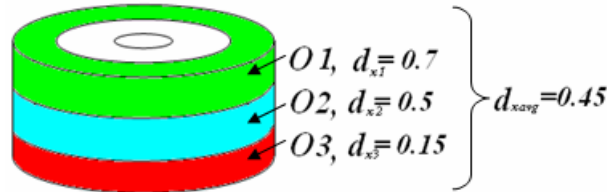

Figure A1 Damage distribution in the outer ellipse.

Solution:

$E_{x1}= E_x(d_{x1})$ is evaluated using a linear interpolation between the two values of damage which are closest to d_{x1} (i.e. d_{xavg} and d_{xf} in this example) as follows:

$$E_{x1}(d_{x1}) = \left[E_x(d_f) - \bar{E}_x\right]\left(\frac{d_{x1} - d_{xavg}}{d_{xf} - d_{xavg}}\right) + \bar{E}_x \tag{A2}$$
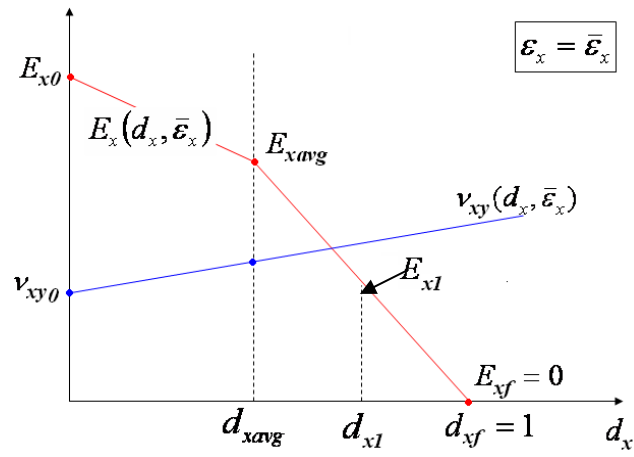
Figure A2

The same procedure can be used to evaluate $E_{x2}(d_{x2})$ and $E_{x3}(d_{x3})$ as well as all the other materials properties $(E_{yi}(d_{yi}), G_{xyi}(d_{xyi})$ with $i=1,2,3)$ except for the Poisson's ratio.